01 Jan 2005

Using a Neural Network to Distinguish Between the Contributions to Harmonic Pollution of Non-Linear Loads and the Rest of the Power System

Joy Mazumdar

Frank C. Lambert

Ganesh K. Venayagamoorthy
Missouri University of Science and Technology

Ronald G. Harley

Recommended Citation

J. Mazumdar et al., "Using a Neural Network to Distinguish Between the Contributions to Harmonic Pollution of Non-Linear Loads and the Rest of the Power System," *Proceedings of the IEEE 36th Power Electronics Specialists Conference, 2005*, Institute of Electrical and Electronics Engineers (IEEE), Jan 2005.
The definitive version is available at https://doi.org/10.1109/PESC.2005.1581862

Using a Neural Network to Distinguish Between the Contributions to Harmonic Pollution of Non-Linear Loads and the Rest of the Power System

Joy Mazumdar, R.G. Harley[1] and F.Lambert
School of Electrical and Computer Engineering
Georgia Institute of Technology
Atlanta, GA 30332-0250, USA
Email: rharley@ece.gatech.edu

Ganesh K. Venayagamoorthy
Real-Time Power and Intelligent Systems Laboratory
Department of Electrical and Computer Engineering
University of Missouri-Rolla
Rolla, MO 65409-0249, USA

Abstract— Harmonics are one of the important power quality measurable quantities. This paper proposes a neural network solution methodology for the problem of measuring the actual amount of harmonic current injected into a power network by a non-linear load. The determination of harmonic currents is complicated by the fact that the supply voltage waveform is distorted by other loads and is rarely a pure sinusoid. Harmonics may therefore be classified as contributions from the load on the one hand and contributions from the power system or supply harmonics on the other hand. A recurrent neural network architecture based method is used to find a way of distinguishing between the load contributed harmonics and supply harmonics, without disconnecting the load from the network. The main advantage of this method is that only waveforms of voltages and currents have to be measured. This method is applicable for both single and three phase loads. This could be fabricated into a commercial instrument that could be installed in substations of large customer loads, or used as a hand-held clip on instrument.

I. INTRODUCTION

The objective of the electric utility is to deliver a sinusoidal voltage at fairly constant magnitude and frequency throughout its network. However, with the widespread proliferation of power electronic loads, significant amounts of harmonic currents are being injected into the network by these loads. When such loads are supplied from a sinusoidal voltage source, their injected harmonic currents are referred to as *contributions from the load.* Fig. 1 shows a simple network structure.

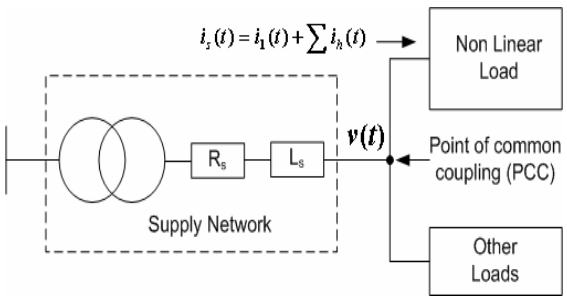

Fig. 1: Simple power system network

The harmonic currents cause harmonic volt drops in the supply network and the voltage at the point of common coupling (PCC) is therefore no longer sinusoidal. Any other loads, even linear loads, connected to the PCC, will have harmonic currents injected into them by the distorted PCC voltage. Such currents are referred to as *contributions from the power system*, or supply harmonics. If the sum of the harmonic currents in the network exceeds a certain limit, it creates problems. Limits of the levels of harmonic currents injected into the system are specified in various standards, guidelines and recommended practices [1,2].

If several loads are connected to a PCC, it is not possible to accurately determine the amount of harmonic current injected by each load, in order to tell which load(s) is injecting the excessively high harmonic currents. If individual harmonic current injections were known, then a utility could penalize the offending consumer in some appropriate way, including say a special tariff or insist on corrective action by the consumer. Simply measuring the harmonic currents at each individual load is not sufficiently accurate since these harmonic currents may be caused by not only the non-linear load, but also by a non-sinusoidal PCC voltage.

This paper proposes a novel method based on Recurrent Neural Networks (RNNs) to distinguish between the two components of harmonic sources (i.e. load or power system). This will enable standards of harmonic pollution to be enforced by utilities and most importantly improve the power quality. Several methods like DFT/FFT [3], stochastic method [4] and in recent years artificial neural networks (ANNs) [5-9] have been proposed to measure the harmonic content in the load current, or to predict it, but most of them assume a radial feeder supplying a single load through a known feeder impedance, or multiple loads connected to a PCC which has a sinusoidal voltage and with zero impedance in the supply feeder.

II. RECURRENT NEURAL NETWORK

Recurrent neural networks (RNNs) are feedback networks in which the present activation state is a function of the previous activation state as well as the present inputs. Adding feedback from the prior activation step introduces a kind of memory to the process. Thus adding recurrent connections to a multilayer perceptron network enhances its ability to learn temporal sequences without fundamentally changing the training process. Recurrent networks will, in general, perform better than regular feedforward networks on systems with transients. They may be trained to identify or approximate any desired continuous vector mapping function $f(.)$ over a specified range.

The block diagram of a RNN interconnected with weight matrices W and V is shown in Fig 2. The objective of the

[1] Professor Emeritus, University of KwaZulu - Natal, Durban, South Africa

training is to modify W and V such that the RNN function $g(.,W,V)$ approximates the desired function $f(.)$, so that the error e between the desired function output y and the RNN output $\hat{y}$ is minimal.

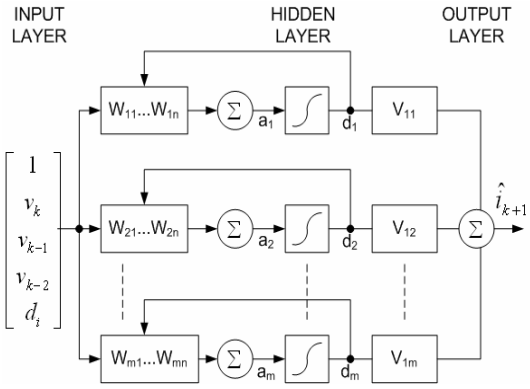

(a)

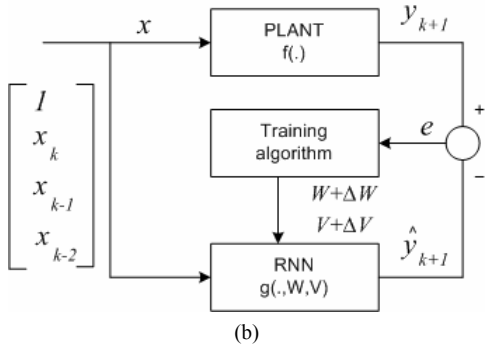

(b)

Fig. 2: (a) RNN architecture; (b) RNN training scheme

Continual online training (COT) is required whenever $f(.)$ is a time varying signal and $g(.,W,V)$ has to track $f(.)$. The online training cycle has two distinct paths: forward propagation and error back-propagation. Forward propagation is the passing of inputs through the neural network structure to its output. Error back-propagation is the passing of the output error to the input in order to estimate the individual contribution of each weight in the network to the final output error. The weights are then modified so as to reduce the output error. The generalized equations are shown below [10].

A. Forward propagation

Every input in the input column vector $\underline{x}$ is fed via the corresponding weight in the input weight matrix W to every node in the hidden layer. The activation vector $\underline{a}$ is determined as the sum of its weighted inputs. In vector notation, this is defined as:

$$\underline{a} = W\underline{x} \tag{1}$$

where the input column vector $\underline{x} \in R^{n+m}$, hidden layer activation column vector $\underline{a} \in R^m$, input weight matrix $W \in R^{m\times(n+m)}$, n is the number of inputs to the RNN including the bias and m is the number of neurons in the hidden-layer.

Each of the hidden node activations in $\underline{a}$ is then passed through a sigmoid function to determine the hidden-layer decision vector $\underline{d}$.

$$d_i = \frac{1}{1+e^{(-a_i)}}, \qquad i \in \{1,2,....,m\} \tag{2}$$

where the decision column vector $\underline{d} \in R^m$.

The decision vector $\underline{d}$ is then fed back to the input layer (this introduces the recurrence) as well as fed to the corresponding weight in the output weight matrix V. The RNN output $\hat{y}$ is computed as

$$\hat{y} = (V\underline{d})^T \tag{3}$$

For a single output system output weight matrix $V \in R^{1\times m}$ and $\hat{y}$ is a scalar.

B. Error back-propagation

The output error e is calculated as

$$e = y - \hat{y} \tag{4}$$

The output error is back propagated through the RNN to determine the errors $\underline{e}_d$ and $\underline{e}_a$ in the decision vector $\underline{d}$ and activation vector $\underline{a}$. The decision error vector $\underline{e}_d$ is obtained by back-propagating the output error e through the output weight vector V;

$$\underline{e}_d = V^T e \tag{5}$$

where the decision error vector $\underline{e}_d \in R^m$.

The activation errors e_{ai} are given as a product of the decision errors e_{di} and the derivative of the decisions d_i with respect to the activations a_i:

$$\begin{aligned} e_{ai} &= \left(\frac{d}{da_i} d_i\right) e_{di} \\ &= \left(\frac{d}{da_i}\left(\frac{1}{1+e^{(-a_i)}}\right)\right) e_{di} \\ &= d_i(1-d_i)e_{di}, \; i \in \{1,2,....,m\} \end{aligned} \tag{6}$$

The derivative of a sigmoidal function can be expressed in terms of its inputs and outputs and computationally it results in multiplication and addition. The subscript i in equation (6) indicates element-wise multiplication of the vectors $\underline{d}$, $\underline{1-d}$ and $\underline{e}_d$.

The change in input weights ΔW and output weights ΔV are calculated as

$$\begin{aligned} \Delta W &= \gamma_m \Delta W + \gamma_g \underline{e}_a \underline{x}^T \\ \Delta V &= \gamma_m \Delta V + \gamma_g \underline{e}_y \underline{d}^T \end{aligned} \tag{7}$$

where $\gamma_m, \gamma_g \in [0,1]$ are the momentum and learning gain constants respectively. The last step in the training process is the actual updating of the weights:

$$\begin{aligned} W &= W + \Delta W \\ V &= V + \Delta V \end{aligned} \tag{8}$$

C. Execution cycle computation

All the necessary equations (1-8) required for the computation of forward propagation and error back-propagation are done in vector form. Most of the computations involve either addition or multiplication. Evaluation of the sigmoidal function is the only computationally demanding task. A complete breakdown of the computations required for one RNN execution cycle is shown in Table 1.

TABLE I
RNN EXECUTION CYCLE COMPUTATIONS

Equation	Multiplication	Addition	Sigmoid
(1)	m(m+n)	m(m+n)	0
(2)	0	0	m
(3)	m	m	0
Forward:	m(m+n+1)	m(m+n+1)	m
(4)	0	1	0
(5)	m	m	0
(6)	2m	0	0
(7): ΔV	2m+1	m	0
(7): ΔW	m(2m+2n+1)	m(2m+2n+1)	0
(8)	0	m(m+n)+m	0
Error back prop	~m(2m+2n+5)	~2m(m+n+1)	0

From the above table it is seen that the forward propagation requires m sigmoidal computations.

III. ESTIMATION OF HARMONIC CURRENT

Figure 3 is a one-line diagram of a three-phase supply network having a sinusoidal voltage source v_s, network impedance L_s, R_s and several loads (one of which is non-linear) connected to a PCC.

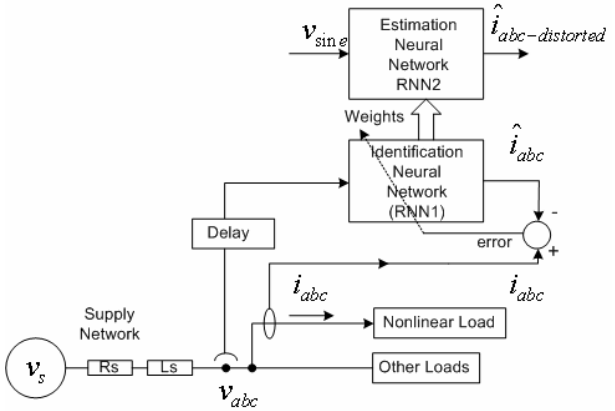

Fig. 3: Proposed scheme

The nonlinear load injects distorted line current i_{abc} into the network. A recurrent neural network is trained to identify the non-linear characteristics of the load. This neural network is called the Identification recurrent neural network (RNN1). A second neural network exists and is called the Estimating recurrent neural network (RNN2). RNN2 is an exact replica of the trained RNN1. Existence of RNN2 enables the simulation action of isolating the load from the network and testing it without physically disconnecting the load from the network. The function of RNN2 can very well be carried out by RNN1, however that would disrupt the continual online training of RNN1 during the brief moments of testing.

A. Identification RNN

The proposed method measures the instantaneous values of the three voltages v_{abc} at the PCC, as well as the three line currents i_{abc} at the k^{th} moment in time. The voltages v_{abc} could be line-to-line or line-to-neutral measurements. The neural network is designed to predict one step ahead line current $\hat{i}_{abc}$ as a function of the present and delayed voltage vector values $v_{abc}(k)$, $v_{abc}(k-1)$ and $v_{abc}(k-2)$. When the $k+1$ moment arrives (at the next sampling instant), the actual instantaneous values of i_{abc} are compared with the previously predicted values of $\hat{i}_{abc}$, and the difference (or error e) is used to train the ANN1 weights. Initially the weights have random values, but after several sampling steps, the training soon converges and the value of the error e diminishes to an acceptably small value. Proof of this is illustrated by the fact that the waveforms for i_{abc} and $\hat{i}_{abc}$ should practically lie on top of each other. At this point the ANN1 therefore represents the admittance of the nonlinear load. This process is called *identifying* the load admittance.

Since continual online training is used, it will correctly represent the load admittance from moment to moment. At any moment in time after the RNN1 training has converged, its weights are transferred to RNN2. The training cycle of RNN1 continues and in this way RNN2 always has updated weights available when needed.

B. Estimation RNN

RNN2 is supplied with a mathematically generated sine wave to estimate its output. The output of RNN2 called $\hat{i}_{abc-distorted}$ therefore represents the current the nonlinear load would have drawn had it been supplied by a sinusoidal voltage source. In other words, this gives the same information that could have been obtained by quickly removing the distorted PCC voltage (if this were possible) and connecting a pure sinusoidal voltage to supply the nonlinear load, except that it is not necessary to actually do this interruption. Any distortion present in the $\hat{i}_{abc-distorted}$ waveform can now be attributed to the nonlinearity of the load admittance.

C. Scaling the RNN variables

Due to the nature of the sigmoidal transfer function, the outputs of the neurons in the hidden layer are limited to values between zero and one. Thus allowing large values for the neuron input variables would cause the threshold function to be driven to saturation frequently and resulting in an inability to train. Hence the network inputs and outputs are normally scaled between zero and one.

IV. EXPERIMENTAL RESULTS

The method of using online trained RNNs to identify the load admittance and testing it is briefly introduced. In most non-linear circuits, some sort of switching power devices are used as the interface between the supply network and the actual load. The performance of the RNN is demonstrated with the help of a simple test setup as shown in Fig. 4.

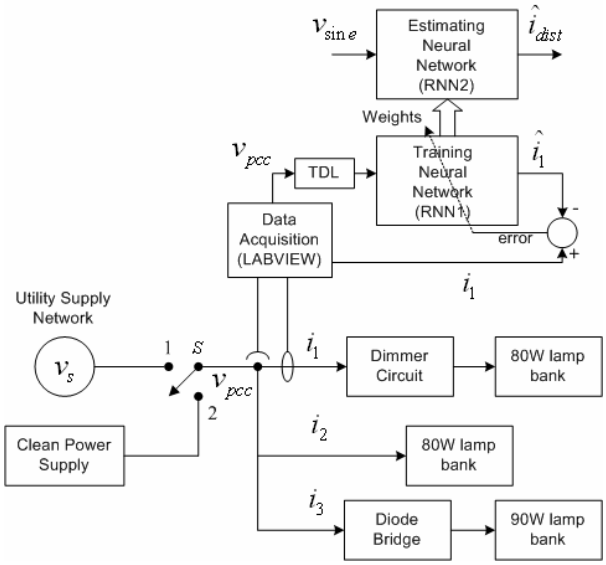

Fig. 4: Experimental setup with 3 loads

The proposed scheme is implemented with three single phase loads connected to a switch S defined as the point of common coupling. The voltage at the PCC is fixed at 120 Vrms, 60 Hz. When S is in position 1, the power supply comes from the utility supply network. When S is in position 2, the power supply comes from a 5 kVA AC clean power source (California Instruments 5000 iX) which provides clean sinusoidal voltage at the point of common coupling (THD < 0.3%).

Load 1: Electronic dimmer circuit supplying an 80 W lamp bank. This is a non-linear load and it's non-linearity depends upon the setting of the firing angle. With 0° firing angle, this load becomes almost linear.

Load 2: 80 W lamp bank connected directly to the PCC. This is a linear load.

Load 3: Full bridge diode rectifier supplying a 90 W lamp bank. This also acts as a linear load due to the lack of inductance in the circuit.

Total Harmonic Distortion is measured by a dedicated spectrum analyzer as well as by data acquisition and MATLAB software. Data acquisition for cases 1 and 2 is carried out with a system from National Instruments and LABVIEW software which stores the data on a personal computer. This data is then imported to MATLAB and using the *powergui* block of SIMULINK, the THD's are computed. These THD's are then compared with measurements taken directly by a spectrum analyzer, in order to verify that the LABVIEW and MATLAB computer code are working correctly. The sampling frequency for data acquisition is 8 kHz which ensures that harmonics up to 4 kHz can be measured. Harmonics above that are normally filtered out by filters.

With the dimmer set to full firing position, two different cases are evaluated with switch S either in position 1 or 2.

Case 1 : Switch S in position 1, dimmer set to 0° firing

The circuit is supplied from the 120 V utility wall socket.

THD of voltage at PCC without any loads = 4.19%
THD of voltage at PCC with all loads connected = 4.24%
THD of current i_1 = 6.11%
THD of current i_2 = 4.25%
THD of current i_3 = 4.32%

Case 2 : Switch S in position 2, dimmer set to 0° firing

The circuit is supplied from the clean power supply.

THD of voltage at PCC without any loads = 0.31%
THD of voltage at PCC with all loads connected = 0.33%
THD of total input current = 1.91%
THD of current i_1 = 4.26%
THD of current i_2 = 0.34%
THD of current i_3 = 0.39%

Now with the dimmer is set to 30° firing, two more cases similar to cases 1 and 2 are evaluated with switch S first in position 1 and then in position 2.

Case 3 : Switch S in position 1, dimmer set to 30° firing

The circuit is supplied from the 120 V utility wall socket.

THD of voltage at PCC without any loads = 4.19%
THD of voltage at PCC with all loads connected = 4.24%
THD of current i_1 = 29.25%
THD of current i_2 = 4.27%
THD of current i_3 = 4.38%

Case 4 : Switch S in position 2, dimmer set to 30° firing

The circuit is supplied from the clean power supply.

THD of voltage at PCC without any loads = 0.31%
THD of voltage at PCC with all loads connected = 0.33%
THD of total input current = 10.1%
THD of current i_1 = 30.42%
THD of current i_2 = 0.37%
THD of current i_3 = 0.4%

An important result is that the current THD of the dimmer circuit is higher when it is being supplied by the clean supply (less THD in v_{pcc}) as compared to when it is supplied by the utility (more THD in v_{pcc}) as shown in cases 3 and 4. However for cases 1 and 2, the result is the other way round. This agrees with the fact that linear loads do not introduce harmonics in the network and do not get affected by the distortion in the supply voltage.

When several loads are supplied from the PCC, with its own background THD, the individual currents are due to the combined effects of the distorted v_{pcc} and the nonlinearities of the loads. This results in some amount of phase cancellation which may reduce the overall harmonic current in the network [11] and thus benefit some of the non-linear loads. Hence, it is essential that the method should be able to analyze every load on its merit [12].

The data obtained from case 1 is used to train the neural network RNN1 until the training error converges to near zero, and the current i_1 of Load-1 correctly tracks the output of RNN1. Figure 5 indicates how well RNN1 has converged since its output $\hat{i}_1$ lies on top of the actual i_1 waveform.

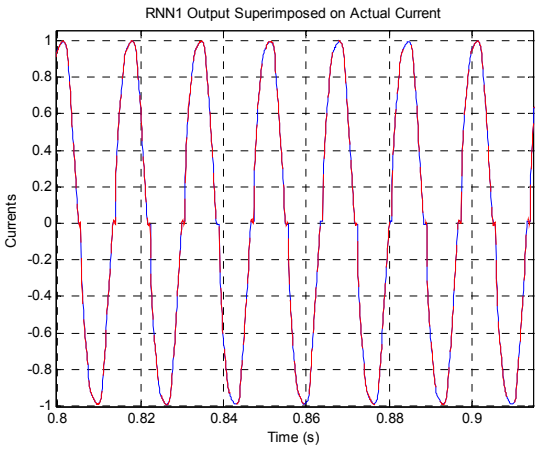

Fig. 5: i_1 and $\hat{i}_1$ superimposed

The convergence of the training can also be verified by looking at the tracking error T_e defined as

$$T_e = i_1 - \hat{i}_1 \tag{9}$$

Once the tracking error is below a pre-defined level, it can be concluded that RNN1 has learned the admittance of Load-1.

The weights of RNN1 are now transferred to RNN2 and is tested with a pure mathematically generated sine wave voltage with zero distortion.

The output of RNN2 is $\hat{i}_{1-dist}$ and it appears in Fig. 6(a) which shows what Fig. 5 would have looked like if it were possible to isolate Load-1 and supplied by a pure sine wave in reality. In other words this is the true harmonic current that would be injected by the non-linear load into the network.

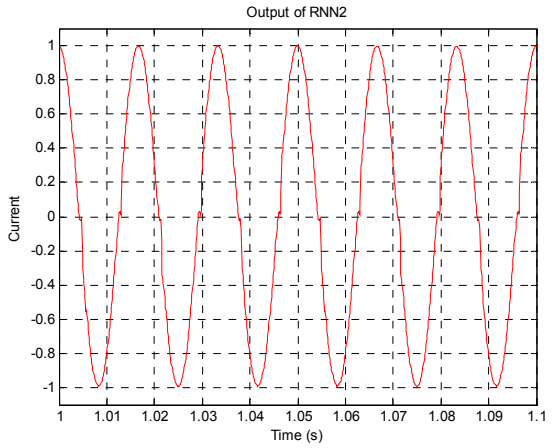

(a)

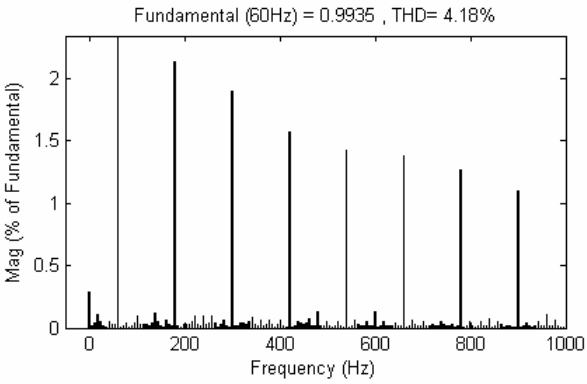

(b)

Fig. 6: (a) $\hat{i}_{1-dist}$ waveform when supplied by pure sine wave and (b) FFT spectrum of $\hat{i}_{1-dist}$. THD=4.18%

The true current THD of $\hat{i}_{1-dist}$ in Fig. 6(b) turns out to be **4.18%** instead of **6.11%** measured in case 1. This result agrees well with the measured value of 4.28% obtained in case 2 where the load was supplied by a 0.3% distorted voltage.

Similarly, the data obtained from case 3 is used to train RNN1 and the convergence result is shown in Fig. 7.

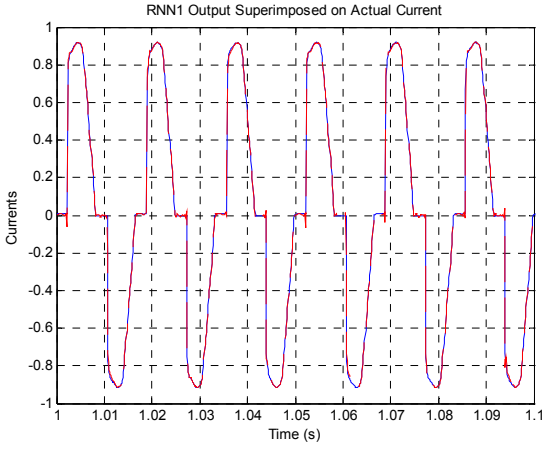

Fig. 7: i_1 and $\hat{i}_1$ superimposed

The weights of RNN1 are transferred to RNN2 and tested with a pure mathematically generated sine wave voltage.

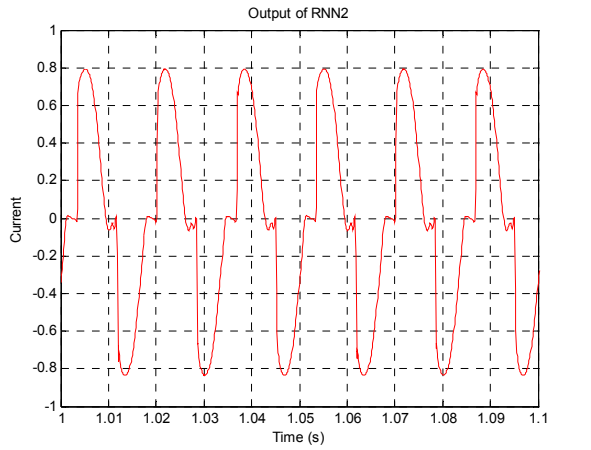

(a)

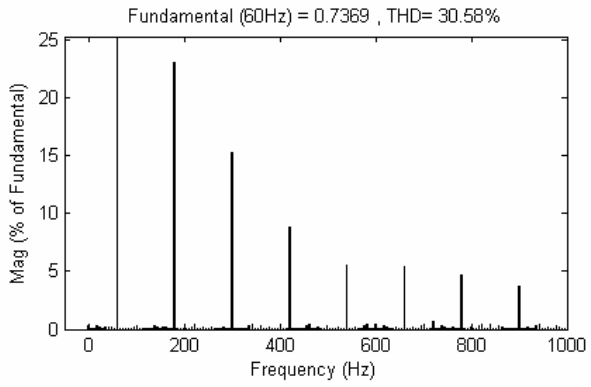

(b)

Fig. 8: (a) $\hat{i}_{1-dist}$ waveform when supplied by pure sine wave and (b) FFT spectrum of $\hat{i}_{1-dist}$. THD=30.58%

The true current THD of $\hat{i}_{1-dist}$ in Fig. 8 turns out to be **30.58%** instead of **29.25%**. This result agrees well with measured value of 30.42% obtained in case 4 where the load was supplied by a 0.3% distorted voltage.

Experiments are also carried out on low voltage systems with diode rectifiers feeding R-L loads as shown in Fig. 9.

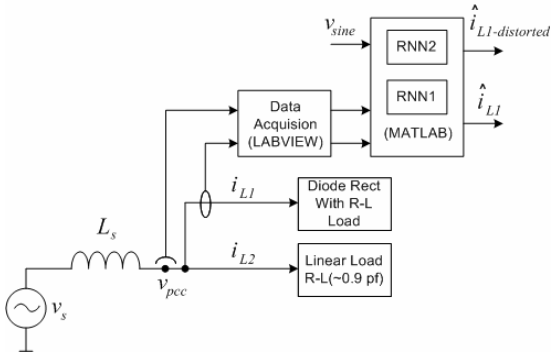

Fig. 9: Experimental setup with low voltage circuits

This scheme is implemented with a single phase diode bridge rectifier feeding an R-L load (Load-1) and a linear R-L load (Load-2), both connected to the PCC. The operating voltage at the PCC is 5 Vrms , 60 Hz which is obtained by using an auto transformer. Each individual load is rated at 1 Amp, and the THD of i_{L1} is 7.8% (measured by signal analyzer), but some of this is due to the non-linearity of Load-1 and some is due to the distortion in the PCC voltage. Without any load connected, the background THD at v_{pcc} is 3.4%. With both loads connected, this THD rises to 6.2%.

With both the loads operating, the current i_{L1} of Load-1 is tracked by RNN1, and the output of RNN1 is $\hat{i}_{L1}$.

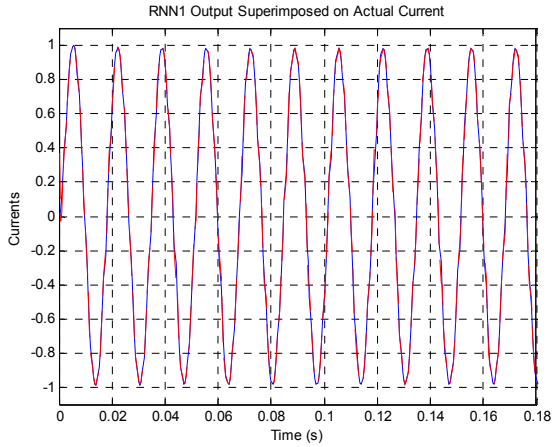

Fig. 10: i_{L1} and $\hat{i}_{L1}$ superimposed

Figure 10 indicates how well RNN1 has converged since its output $\hat{i}_{L1}$ lies on top of the actual i_{L1} waveform. RNN1 has therefore learned the admittance of Load-1.

The weights of RNN1 are now passed to RNN2 which is supplied from a mathematically generated sine wave voltage with zero distortion. The output $\hat{i}_{L1-distorted}$ from RNN2 is plotted in Fig. 11and shows what Fig. 10 would have looked like if the voltage v_{pcc} had no distortion.

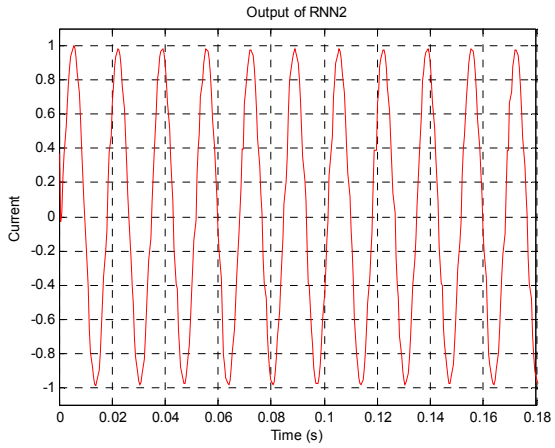

Fig. 11: $\hat{i}_{L1-distorted}$ waveform when supplied by a mathematically generated sine wave

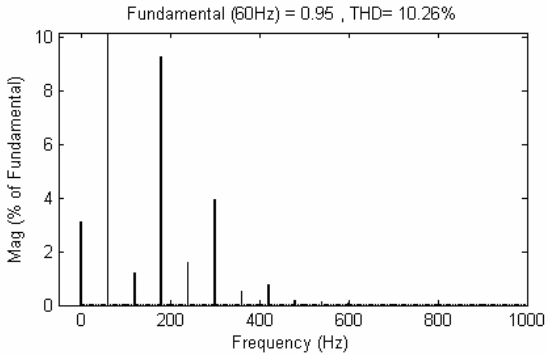

Fig. 12: FFT spectrum of $\hat{i}_{L1-distorted}$. THD=10.26%

The THD of $\hat{i}_{L1-distorted}$ as shown in Fig. 12 is now **10.26%** instead of **7.8%**. This means that the true current THD of Load-1 is higher that what was measured when it was a part of the power network.

The salient results of the three experiments performed are summarized in Table I.

TABLE II
SUMMARY OF RESULTS

Load	THD_d	THD_s	$e_m = \left(\frac{THD_s - THD_d}{THD_s} \right)$
Dimmer-Full setting	6.11%	4.18%	-46.17%
Dimmer-3/4th setting	29.25%	30.58%	4.35%
Bridge Rectifier	7.68%	10.26%	-25.15%

where THD_d is i_{THD} from distorted v_{pcc} and THD_s is i_{THD} from pure sine wave. A new parameter e_m known as the resultant error in measurement is introduced above and can be used as an indicator of the error in the measurement if the calculation of THD is done just by measuring the input current of the non-linear load.

One important finding from the above results show that it is erroneous to think intuitively that the current THD, when supplied from a distorted v_{pcc} should always be higher than if the v_{pcc} had no distortion.

A. Recurrent neural network details

Some of the experimental details of the RNN implementation are given below:

- Recurrent neural network implemented in MATLAB
- FFT computation : *powergui* block of SIMULINK
- Number of Neurons in the hidden layer: 20.
- Time delayed inputs : 2
- Learning gain : 0.05. Momentum gain not used

V. CONCLUSION

Non-linear loads exhibit customer contributed harmonics. Linear loads draw distorted currents because of a distorted v_{pcc} caused by non-linear loads. However in an actual network, loads cannot be isolated. Therefore it is impossible to say which load is causing the pollution and which load is suffering from the pollution. The novel method described in this paper avoids disconnecting any loads from the system and estimates the actual harmonic current injected by each load. This information could be used to penalize the offending load.

The biggest advantage of this method is that only waveforms of voltages and currents have to be measured. On a practical system the neural network computations can be carried out on a DSP, together with a suitable A-D interface. Such a system could be installed permanently or be portable from one customer to another in order to simply monitor pollution levels at a particular PCC in the network.

ACKNOWLEDGMENT

Financial support by the National Electric Energy Testing Research and Applications Center (NEETRAC), USA; and from the Duke Power Company, Charlotte, North Carolina, USA, for this research is greatly acknowledged.

REFERENCES

[1] IEEE Power System Harmonic Working Group, "Bibliography of Power System Harmonics, Part I and II", *IEEE PES Winter Power Meeting,* Paper 84 WM 214-3, Jan. 29-Feb. 3, 1984.

[2] IEEE Standard 519-1992, IEEE Recommended Practices and Requirements for Harmonic Control in Electric Power Systems.

[3] T. A. George, and D. Bones, "Harmonic power flow determination using the fast Fourier transform", *IEEE Transactions on Power Delivery*, Volume: 6 Issue: 2, April 1991, pp. 530 –535.

[4] Y. Baghzouz, and O. T. Tan, "Probabilistic Modeling of Power System Harmonics", *IEEE Transactions on Industry Applications*, Vol, IA-23, No. 1, January/February 1987, pp. 173-180.

[5] H. Mori, and S. Suga, "Power system harmonics prediction with an artificial neural network", *IEEE International Symposium on Circuits and Systems*, 11-14 June 1991, Vol. 2, pp. 1129 –1132.

[6] M. Rukonuzzaman, A.A.M Zin, H. Shaibon, and K. L. Lo, "An application of neural network in power system harmonic detection", *IEEE World Congress on Computational Intelligence. The 1998 IEEE International Joint Conference on Neural Networks*, Vol. 1, 4-9 May 1998, pp. 74 –78.

[7] S. Osowski, "Neural network for estimation of harmonic components in a power system", *IEE Proceedings on Generation, Transmission and Distribution*, Vol. 139, Issue 2, March 1992, pp. 129 – 135.

[8] W.W.L Keerthipala, Low Tah Chong and Tham Chong Leong, "Artificial neural network model for analysis of power system harmonics", *IEEE International Conference on Neural Networks, 1995*, 27 Nov.-1 Dec. 1995, Vol.2, pp. 905 – 910.

[9] N. Pecharanin, H. Mitsui, and M. Sone, "Harmonic detection by using neural network", *IEEE International Conference on Neural Networks, 1995*, 27 Nov.-1 Dec. 1995, Vol.2, pp. 923 – 926.

[10] B. Burton and R.G. Harley, "Reducing the computational demands of continually online-trained artificial neural networks for system identification and control of fast processes", *IEEE Transactions on Industry Applications*, Vol. 34 , Issue: 3, May-June 1998 pp. 589 – 596.

[11] W.M. Grady, A. Mansoor, E.F. Fuchs, P. Verde amd M. Doyle, "Estimating the net harmonic currents produced by selected distributed single-phase loads: computers, televisions, and incandescent light dimmers", *IEEE Power Engineering Society Winter Meeting, 2002*, Vol. 2 , 27-31 Jan. 2002, pp. 1090 – 1094.

[12] C.R. van Niekerk, A.P.J. Rens and A.J. Hoffman, "Identification of types of distortion sources in power systems by applying neural networks", *6th IEEE AFRICON*, 2-4 Oct. 2002, Vol. 2, pp. 829 – 834.